

# INVESTIGATION OF AEROSOLS SPREADING CONDITIONS IN ATMOSPHERE USING REMOTE SENSING DATA AND NON-HYDROSTATIC METEOROLOGICAL NUMERICAL MODELS DATA

I. A. Winnicki\*, K. Kroszczynski, J. M. Jasinski, S. Pietrek

Faculty of Civil Engineering and Geodesy, Military University of Technology Kaliskiego 2 Str., 00-908 Warsaw, Poland -(ireneusz.winnicki@wat.edu.pl, janusz.jasinski@wat.edu.pl, rwkk@op.pl, spietrek@wat.edu.pl)

Commission VIII, WG VIII/3

**KEY WORDS:** Satellite remote sensing, Modelling, Image understanding, Simulation, Air Pollution, Prediction.

## ABSTRACT:

Two ways of aerosols spreading analysis in atmosphere are presented. The first one is based on the one-level barotropic models. This case includes the simple tests of the numerical simulations spreading of a clouds of contaminants in free atmosphere. The solutions for this example was obtained using the non-divergent equation of the quasi-solenoidal or quasi-geostrophic models in the barotropic approaches. The considered equation is a nonlinear differential equation of Monge-Ampere (MA) type used for determining a streamfunction field when the geopotential field is known. It is obtained by transforming the governing equations and assuming that the divergence of wind field is equal to zero. The nonlinear balance equation is a part of the general system equations describing quasi-solenoidal or quasi-geostrophic models. The second way of the analysis is based on the COAMPS (Coupled Ocean/Atmosphere Mesoscale Prediction System) non-hydrostatic numerical weather prediction model developed by Naval Research Laboratory, Monterey, California (Hodur, 1997). This multi-level numerical weather forecasting model is tested in the Applied Geomatics Section, MUT. Research results are presented and discussed with students of geoinformatics and meteorology. Weather forecast for Poland is presented every day on the Faculty's web-page. The main equation describing the propagation process – the aerosol-tracer continuity equation is derived from the mass flux form of the conservation equation. This form of the continuity equation conserves the mass. In COAMPS, the 3D continuity equation is integrated forward in time with three equivalent one-dimensional equations (time splitting method). Both the explicit and implicit numerical methods for integration in time are available to solve the diffusion expressions in the continuity equation. The COAMPS nested grid model run on the IA64x32 Feniks cluster with the three-dimensional aerosol-tracer module. This model is executed in Poland in order to recognize the distribution of tropospheric aerosol and chemical conditions for the first time. The Mazovian Province digital terrain model (DTM) is taken into consideration. In this case the simulations of the propagation of gas pollution emitted by the four Warsaw Power Plant chimneys: Wola, Kaweczyn, Siekierki and Zeran are presented. The chosen analysis also include the pollution from the Steelworks Warsaw (west part of the capitol).

## 1. INTRODUCTION

On the base of real measurement data (geopotential of the isobaric 500 hPa surface) obtained from the GRID data sets the barotropic model in quasi-solenoidal approach is solved. The method of analysis of the point-source gas pollutant propagation in the barotropic atmosphere is presented. The wind components are defined as a streamfunction. Solutions of some numerical simulations are presented. The nonlinear balance equation is a part of the general system equations describing quasi-solenoidal or quasi-geostrophic models.

## 2. PRIMITIVE EQUATIONS AND DIFFUSION

### 2.1 Primitive Equations

The numerical weather forecasting process based upon the non-divergent models in barotropic approaches can be divided into three following stages:

1. Computing the horizontal components of the wind velocity (the geostrophic model) or the stream-function field (the

solenoidal model) treating the geopotential as known data – solution of the balance equation.

2. Predicting of the geopotential field (quasi-geostrophic model) or the streamfunction field (the quasi-solenoidal model) for 12 or 24 hours, for instance, and
3. Solving the balance equation for geopotential or streamfunction. In the quasi-geostrophic model, on the basis of the prognostic geopotential field, we obtain a prognostic wind field. In the quasi-solenoidal model, on the basis of prognostic streamfunction we obtain a prognostic geopotential field.

For the realization of the first stage of the weather forecasting process it is necessary to analyze a non-linear balance equation for streamfunction  $\psi$ , a particular case of Monge-Ampere (MA) equation type. It is a diagnostic equation. Because of the nonlinearity, an iterative solution procedure must be used. The main point is that if it lead to a convergent sequence of solution they have to satisfy the general condition of a convergence of the Monge-Ampere equation. That condition depends mostly on the geometry of the geopotential field. The curvature of this field must be elliptic. It is an ellipticity criterion of the balance equation. Let us consider a system of barotropic primitive

---

\* Corresponding author.

equations, known as the shallow water model. It can be written in Cartesian coordinates:

$$\begin{aligned} \frac{\partial u}{\partial t} + u \frac{\partial u}{\partial x} + v \frac{\partial u}{\partial y} &= -\frac{\partial \Phi}{\partial x} + fv \\ \frac{\partial v}{\partial t} + u \frac{\partial v}{\partial x} + v \frac{\partial v}{\partial y} &= -\frac{\partial \Phi}{\partial y} - fu \\ \frac{\partial \Phi}{\partial t} + u \frac{\partial \Phi}{\partial x} + v \frac{\partial \Phi}{\partial y} + \Phi \left( \frac{\partial u}{\partial x} + \frac{\partial v}{\partial y} \right) &= 0 \end{aligned} \quad (1)$$

where:  $\Phi = gH$  – geopotential, ( $H$  – the free surface height),  
 $u, v$  – are the components of the wind vector along the  $x$  and  $y$  axes of the coordinate Cartesian system,  
 $g$  – gravity acceleration,  
 $f$  – Coriolis parameter,  $f = 2\omega \sin \varphi$ ,  
 $\varphi$  – latitude.

This transformation leads to the vorticity equation for  $\nabla^2 \psi$ :

$$\frac{\partial \nabla^2 \psi}{\partial t} + u \frac{\partial (\nabla^2 \psi + f)}{\partial x} + v \frac{\partial (\nabla^2 \psi + f)}{\partial y} = -(\nabla^2 \psi + f) \left( \frac{\partial u}{\partial x} + \frac{\partial v}{\partial y} \right) \quad (2)$$

where streamfunction  $\psi$  is defined by the relations:

$$u_\psi = -\frac{\partial \psi}{\partial y} \quad v_\psi = \frac{\partial \psi}{\partial x} \quad (3)$$

Let us turn the attention to the real atmospheric motions. They usually consist small perturbations. One can describe them as:

$$u = u_\psi + u' = -\frac{\partial \psi}{\partial y} + u' \quad v = v_\psi + v' = \frac{\partial \psi}{\partial x} + v' \quad (4)$$

where:  $u', v'$  – fluctuations in the  $x$  and  $y$  directions.

Substituting (4) for (2) and neglecting the terms of lower order one can obtain:

$$\frac{\partial \nabla^2 \psi}{\partial t} - \frac{f}{\psi} \frac{\partial \psi}{\partial t} J(\nabla^2 \psi + f, \psi) = 0 \quad (5)$$

For the sake of simplicity it is suggested to treat the streamfunction  $\psi$  in the denominator of the coefficient at the time derivative as a constant value being the mean value over the considered area. Hence

$$\bar{\psi} = \frac{1}{M \cdot N} \sum_{i=1}^M \sum_{j=1}^N \psi_{ij} \quad (6)$$

where:  $M, N$  – number of grid points along  $x$  and  $y$  axes. Finally we obtain

$$\frac{\partial \nabla^2 \psi}{\partial t} - \frac{f}{\bar{\psi}} \frac{\partial \psi}{\partial t} J(\nabla^2 \psi + f, \psi) = 0 \quad (7)$$

or

$$\nabla^2 q - \alpha^2 q = J(\nabla^2 \psi + f, \psi) \quad (8)$$

where:  $q = \partial \psi / \partial t$  – the streamfunction tendency,  
 $\alpha^2 = f / \bar{\psi}$  – parameter.

With respect to  $q$  (8) is Helmholtz equation. Meteorologists call it barotropic divergent model in quasi-solenoidal approach or generalized vorticity equation. In Figure 1 the contour plots of 500 hPa height data (input geopotential data) obtained from the meteorological measurements are shown. In Figure 2 the contour plots of wind velocity for the analysed geopotential field is illustrated.

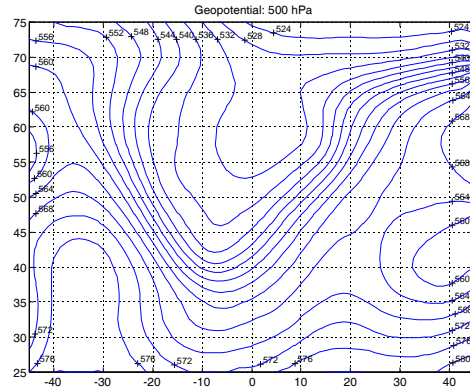


Figure 1. Input geopotential  $\Phi$  field (measured data).

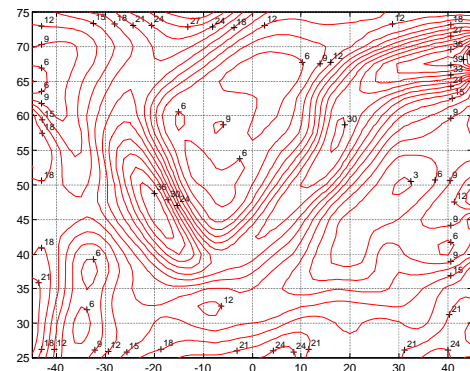


Figure 2. Wind velocity field of the 500 hPa level.

## 2.2 The Balance Equation

The Monge–Ampere equation is a second order nonlinear partial differential one, which can be written in general form

$$r \cdot t - s^2 = a \cdot r + 2b \cdot s + c \cdot t + g \quad (9)$$

where:

$$r = \frac{\partial^2 \psi}{\partial x^2} \quad s = \frac{\partial^2 \psi}{\partial x \partial y} \quad t = \frac{\partial^2 \psi}{\partial y^2} \quad (10)$$

Its coefficients  $a, b$  and  $c$  depend on  $x, y$ , the sought-for function and its first derivatives

$$p = \frac{\partial \psi}{\partial x} \quad q = \frac{\partial \psi}{\partial y}$$

where:  $p, q$  – Monge's symbols.

Let us present the final form of the balance equation as

$$\frac{\partial^2 \psi}{\partial x^2} \cdot \frac{\partial^2 \psi}{\partial y^2} - \left( \frac{\partial^2 \psi}{\partial x \partial y} \right)^2 + a \cdot \frac{\partial^2 \psi}{\partial x^2} + 2b \cdot \frac{\partial^2 \psi}{\partial x \partial y} + c \cdot \frac{\partial^2 \psi}{\partial y^2} + g = 0 \quad (11)$$

where:  $a = c = \frac{f}{2}$   
 $b = 0$

$$g = -\frac{1}{2} \nabla^2 \Phi + \frac{1}{2} \left( \frac{\partial \psi}{\partial x} \frac{\partial f}{\partial x} + \frac{\partial \psi}{\partial y} \frac{\partial f}{\partial y} \right)$$

Solving the balance equation for streamfunction we obtain the prognostic wind field and next one can solve the advection – diffusion two – dimensional problem (red closed lines in the Figure 3 through Figure 5).

The MA equation may be of elliptic, hyperbolic or parabolic type. The type depends on the sign of expression

$$\Delta = (2 \cdot \nabla^2 \Phi = f^2) / 4 \quad (12)$$

which is called an ellipticity criterion for MA equation. If  $\Delta > 0$  the MA equation is of elliptic type. In the opposite case it is hyperbolic and if  $\Delta = 0$  the MA equation is of parabolic type. The solution of the equation (11) is physically acceptable only when it is of elliptic type (Winnicki, 1995).

The criterion (12) depends strongly on the sign of  $\nabla^2 \Phi$  and relations between the geopotential field and Coriolis parameter  $f$ . In the real atmosphere the condition of ellipticity  $\Delta = (2 \cdot \nabla^2 \Phi = f^2) / 4 > 0$  is usually satisfied in the high and mid-latitudes for majority atmospheric situations, including anticyclones and atmospheric fronts. In spite of the  $\nabla^2 \Phi < 0$ , the criterion  $2 \cdot \nabla^2 \Phi + f^2 > 0$  is true. In the area of low pressure (cyclones) due to the relation  $\nabla^2 \Phi > 0$  the ellipticity condition is always satisfied. It does not depend on the latitude. For low latitudes criterion (12) is not satisfied for anticyclones with high anticyclonic curvature and the modification of geopotential field is obligatory. The function  $f^2$  reaches 0 very fast. The observation data sometimes need to be modified to satisfy the ellipticity criterion of the balance equation.

### 2.3 Advection – Diffusion Equation for the Quasi-Solenoidal Approach

The diffusion equation with advection terms solved here can be written as follows

$$\frac{\partial C}{\partial t} + u \frac{\partial C}{\partial x} + v \frac{\partial C}{\partial y} - K_{xy} \left( \frac{\partial^2 C}{\partial x^2} + \frac{\partial^2 C}{\partial y^2} \right) = Q(x, y, t) \quad (13)$$

where:  $C$  – concentration of the gas pollutant,  
 $K_{xy}$  – the kinematics coefficients of eddy viscosity for horizontal eddies,  
 $Q(x, y, t)$  – the point-source gas pollutant emission rate (mass per unit time).

### 2.4 Numerical simulations

**Note:** The choice of sources localization was accidental. It was strictly connected with geopotential and wind fields over the Europe and North Atlantic, which were included into considerations. For the calculations the first source was placed at the start of the convergence zone over the Atlantic Ocean, the second – at its end (North Africa).

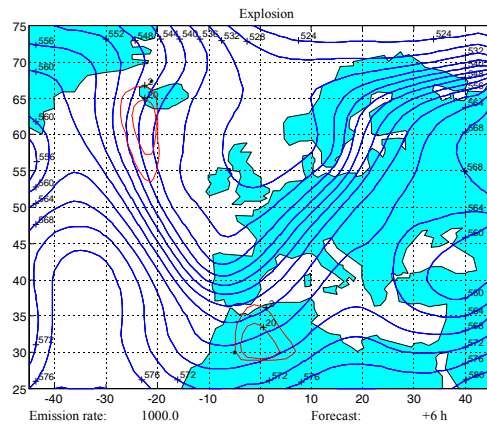


Figure 3. Simulation after 6 hours.

Two point-sources (e.g. nuclear plants) are located in the considered area. Its coordinates are (66°N, 20°W) – Iceland and (30°N, 6°W) – Morocco. The stars show their positions. The first source of pollution there is in the area of very strong wind (see Figure 2). Considered plant is located on the edge of the convergence zone. The propagation process runs very fast. The range of contamination is growing to the south of the Atlantic Ocean reaching the south part of the Spain and Morocco (see Figure 3 through Figure 5).

The second plant is located at the edge of the divergence zone. The propagation process runs slower. The range of contamination does not grow so fast.

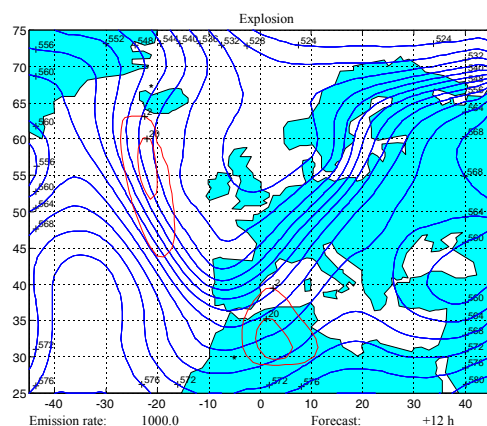


Figure 4. Simulation after 12 hours.

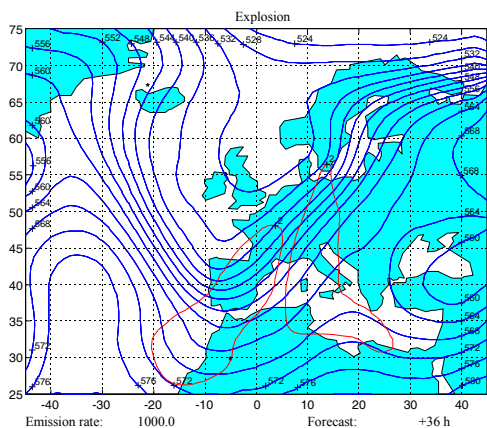


Figure 5. Simulation after 36 hours.

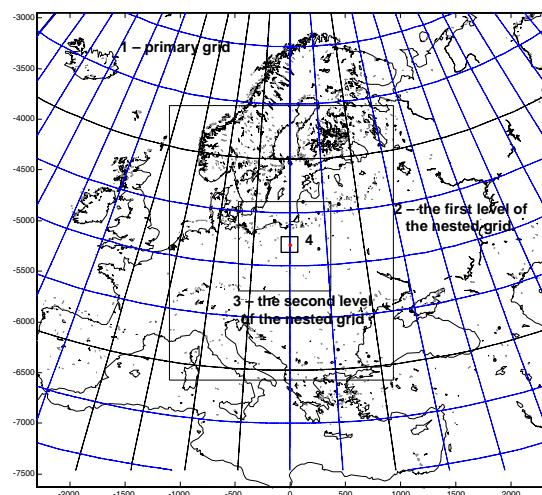


Figure 6. Telescopic multi-nested calculation grid

### 3. THE COAMPS AEROSOL-TRACER MODULE

#### 3.1 Introduction

The increasing level of atmosphere pollution caused by the development of industry, mass-production, transportation, extraction of resources and influence of urban areas affects greatly the natural environment. During the previous century the natural environment was subject to a vast change. The greenhouse effect, ozone hole, acid rain, decrease in forest areas, electromagnetic smog, are only a part of the present ecological threats caused by human. This is why conducting research studies concerning the emission and propagation of gas pollution is vital. The Ministry of the Environment decree (dated 13 June 2003), concerning the measuring of emission levels, defines the official requirements regarding the continuous measurements of gaseous pollutant emission levels, which must be conducted above all by heat and power plants, steelworks and plants emitting air organic pollutants. The Directive 2001/81/WE of the European Parliament and of the Council (dated 23 October 2001) makes it obligatory for all the EU nations to reduce by 2010 their annual emission of sulfur dioxide, nitrous oxides, gaseous organic compounds and ammonia to the levels defined in the Directive. The research conducted by Applied Geomatics Section concern the distribution of gases (CO<sub>2</sub>, N<sub>2</sub>O, NO<sub>x</sub>, SO<sub>2</sub>, H<sub>2</sub>S, aromatic compounds), aerosols and dusts (radioactive wastes), which constitute the main source of pollution.

The future studies including the introduction of more advanced parameterization of the COAMPS model (i.e. adjusted numerical model or modified algorithm of the turbulence and planetary boundary layer) will cover also the pollution caused by ground vehicle transportation, chemical industry and dispersed energy sources (NO<sub>x</sub>, SO<sub>2</sub>, dusts).

Meso- and microscale models will enhance monitoring of chemical, biological or radiological contamination threats resulting from events such as technical damages, catastrophes, natural disasters or terrorist attacks. The models will also facilitate creation of possible contamination scenarios ensuring the ability to identify areas threatened with pollution concentration. In cases of emergency, sufficient information about the speed and direction of pollution spreading is critical to minimize risk to residents of threatened areas as well as to rescue teams.

The COAMPS model is not here described precisely (for more details see Hodur, 1997). COAMPS runs on the nested grid methodology. Nested grid methodology (Figure 6) is used in parallelized calculation process. This process is designed to facilitate two way interaction in which the boundary and initial conditions and state parameters, including pollution concentration, may flow from the grid with large spatial step to the sub-grid. It is possible also that the smaller scale processes may affect the pollution propagation in the larger areas.

#### 3.2 The Continuity Equation

The continuity equation written in the conservative form, i.e.:

$$\frac{\partial C}{\partial t} + \frac{\partial(uC)}{\partial x} + \frac{\partial(vC)}{\partial y} + \frac{\partial[(d\sigma/dt + v_f)C]}{\partial \sigma} = D_x - D_y - D_\sigma - C_{src} + C_{snk} \quad (14)$$

is the three-dimensional partial differential one of the parabolic type.  $C$  represents the mass concentration (kg m<sup>-3</sup>) as defined by the COAMPS transformed coordinate. The horizontal velocity components of  $x$  and  $y$  directions ( $u$  and  $v$ ) and the particle gravitational fall velocity  $v_f$  are scaled separately by the horizontal map scaling factors at the staggered velocity-grid points and by the  $\sigma$ -coordinate scaling factor

$$z_m = (z_{top} - z_{sfc}) / z_{top} \quad (15)$$

where:  $C_{src}$  is the source and  $C_{snk}$  is the sink aerosols or tracers represented in units of km<sup>-3</sup> s<sup>-1</sup>.

The source concentration term may represent any of the following:

- injection of aerosol particles,
- formation of new particles by nucleation,
- tracer emission.

The sink concentration term may represent a parameterized precipitation removal, surface deposition, or other processes (e.g., heterogeneous nucleation). The terms  $D_x$ ,  $D_y$ , and  $D_\sigma$  all

represent subgrid scale turbulent mixing in the  $x$ ,  $y$ , and  $\sigma$  directions. The abovementioned terms are defined as follows:

$$D_x = \frac{\partial}{\partial x} \left( K_x \frac{\partial C}{\partial x} \right) \quad D_x = \frac{\partial}{\partial x} \left( K_x \frac{\partial C}{\partial x} \right) \quad (15)$$

$$D_\sigma = \left( \frac{z_{top}}{z_{top} - z_{sfc}} \right)^2 \frac{\partial}{\partial \sigma} \left( K_\sigma \frac{\partial C}{\partial \sigma} \right) \quad (16)$$

where:

$$\sigma = z_{top} \frac{z - z_{sfc}}{z_{top} - z_{sfc}}$$

It is general vertical coordinate, augmented with the COAMPS terrain-following sigma coordinate. In the sigma formula,  $z$  is the vertical altitude,  $z_{top}$  is the depth of model domain, and  $z_{sfc}$  is the terrain height at the grid points.

### 3.3 Vertical structure of the COAMPS

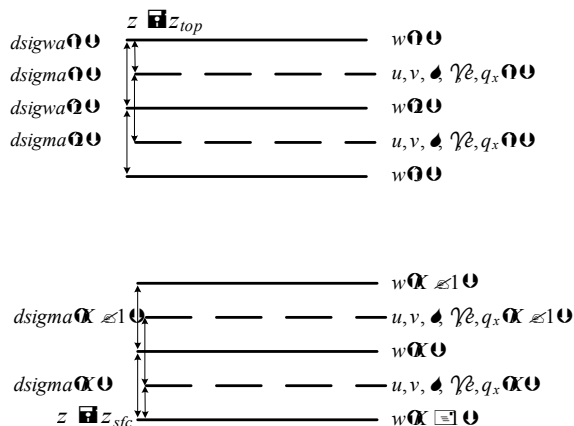


Figure 7. The vertical structure of the COAMPS.

COAMPS includes 30 levels of data, but it is possible to increase the number of levels by about 10. For the analysis of the gas pollution spreading the most important layer is the ground level – 1600m. In this range we have the following heights (in [m]):

- 0.0; 10.0; 20.0; 30.0; 40.0; 55.0; 70.0; 90.0; 110.0; 140.0;
- 170.0; 215.0; 260.0; 330.0; 400.0; 500.0; 600.0; 750.0; 900.0;
- 1100.0; 1300.0; 1600.0

### 3.4 The numerical simulations

The several numerical simulations were carried out on the base of COAMPS. They include the Warsaw area (Figure 8) and the Mazovian Province area. The quantities of the emitted pollution were not taken from reports officially published by the power plants and steelworks supervisory boards. They were assumed for the calculations needs only. Authors do not take the responsibility for publishing by other persons results of tests presented here.



Figure 8. Warsaw Power Plants (Google™).

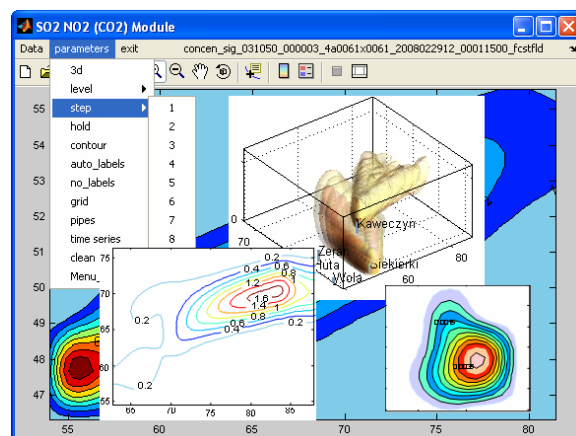


Figure 9. The system for time – spatial analysis.

### 3.5 Data analysis

The data can be interpolated on the locally parallel surfaces. Additionally, the presented module can deliver information on weakening of the stream (extinction factor) and the radiation optical length. Due to a very large amount of output data, a dedicated application for analysis (Figure 9) was developed in the Applied Geomatics Section. The application enables:

- simultaneous tracing of pollution propagation and weather changes for different sub-areas of Europe (functionality for defining calculation grids),
- analysis of the non-stationary distributions of volume and surface pollution for every single emitter and a combined group of emitters,
- detection of concentration levels exceeding the allowed ones,
- measuring the influence of meteorological conditions: inversion (sedimentation of pollution near the emitters), convection (long-range transportation), deposition (dry and wet),
- uniform data processing system and their registration, archivization and sharing.

### 3.6 Meteorological conditions

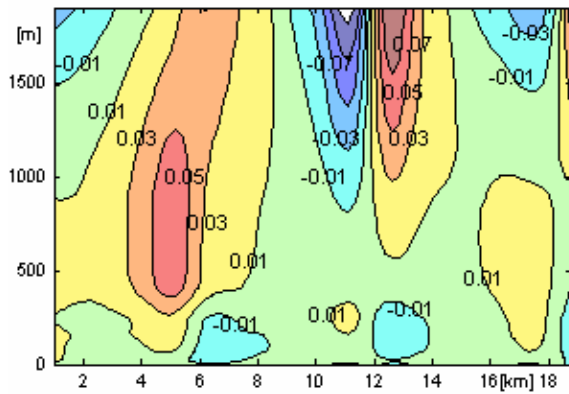


Figure 10. Vertical motion field over the Mazovian Province, 29.02.2008 – weak convection, in  $[m\ s^{-1}]$ .

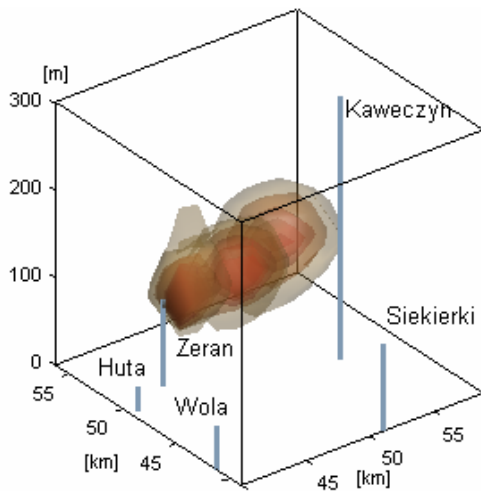


Figure 11. Vertical range of gas pollutions in the weak convection conditions (29.02.2008). The smoke trail reaches 300m level.

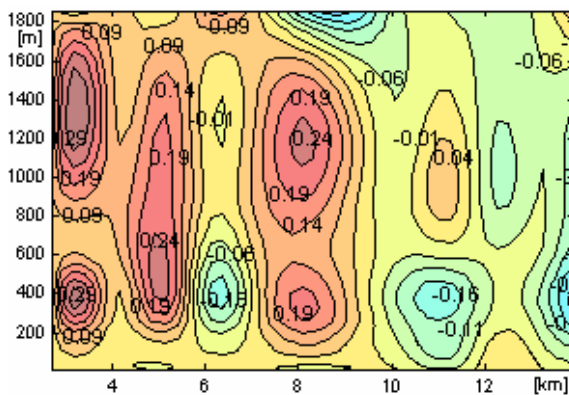


Figure 12. Vertical motion field over the Mazovian Province, 18.04.2008 – strong convection, in  $[m\ s^{-1}]$ .

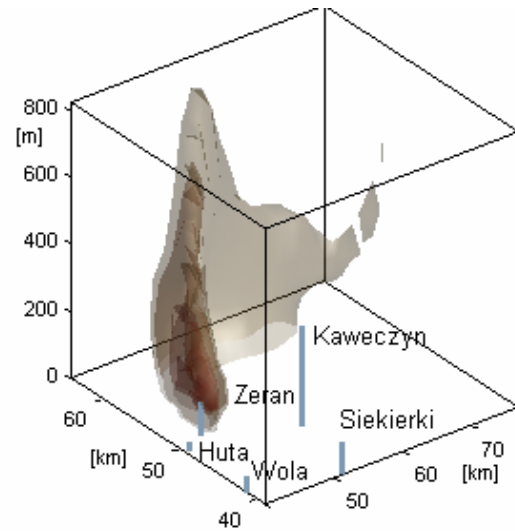


Figure 13. Vertical range of gas pollutions in the strong convection conditions (18.04.2008). The smoke trail reaches 800m level.

The figures presented above illustrate two meteorological situations: weak and strong convection. The vertical distributions of gas pollution emitted by Warsaw Power Plants are different.

The strong convection shortens the horizontal range of the propagation process. However, the weak convection causes that the horizontal range is visibly larger, and the contaminants concentration decompose on the larger area, too.

### REFERENCES

- Hodur, R.M., 1997. The Naval Research Laboratory's Coupled Ocean/Atmosphere Mesoscale Prediction System (COAMPS), *Mon. Wea. Rev.*, **135**, pp. 1414–1430.
- Winnicki, I., 1995, The ellipticity condition of the Monge – Ampere equation in the solenoidal model., *J. Techn. Phys.*, **36**, pp. 299 – 315.

### ACKNOWLEDGEMENTS

This study is supported by the Ministry of Science and Higher Education, Poland: Grant No O N306 0033 33 – *Non-hydrostatic mesoscale models data application to meteorological support of Air Force operations.*